Thin Solid Films 550 (2014) 121–127

Contents lists available at ScienceDirect

Thin Solid Films

journal homepage: www.elsevier.com/locate/tsf

Structural, optical, photoluminescence and photocatalytic investigations on Fe doped TiO_2 thin films

Prabitha B. Nair [a], V.B.Justinvictor [a], Georgi P. Daniel [a], K. Joy [a], V. Ramakrishnan [b], David Devraj Kumar [c], P.V. Thomas [a,*]

[a] Thin Film Lab, Post Graduate and Research Department of Physics, Mar Ivanios College, Nalanchira, Thiruvananthapuram 695015, Kerala, India
[b] Department of Laser Studies, School of Physics, Madhurai Kamaraj University, Madurai 625021, Tamilnadu, India
[c] College of Education, Florida Atlantic University, 3200 College Avenue Davie, FL 33314, USA

ARTICLE INFO

Article history:
Received 17 October 2012
Received in revised form 17 October 2013
Accepted 18 October 2013
Available online 30 October 2013

Keywords:
Iron
Titanium dioxide
Sputtering
Micro Strain
Dislocation Density
Band Gap
Photoluminescence
Photocatalytic Activity

ABSTRACT

Pure and Fe doped TiO_2 thin films were deposited onto quartz substrates maintained at room temperature by radio frequency magnetron sputtering. The films were annealed at 873 K in air for 2 h and characterized using X-ray diffraction (XRD), micro Raman spectroscopy, Scanning electron microscopy (SEM), Energy dispersive spectroscopy, ultraviolet-visible and photoluminescence (PL) spectroscopy. Pure TiO_2 thin films were XRD-amorphous, but micro Raman spectra revealed the presence of anatase phase. Doping with Fe has influenced the transformation of films to anatase phase. Improved crystallinity was observed in the 0.1 at% Fe doped films, where the lattice constants approached the values for bulk anatase TiO_2, and the films showed minimum strain. At higher Fe concentrations, micro Raman spectra revealed the presence of rutile phase also. SEM images revealed crack free surface and surface roughness was found to increase with increase in Fe concentration. Doping with Fe has resulted in a red shift of absorption edge. PL emission intensity was found to increase with Fe concentration, but at higher concentrations quenching of PL emission was observed. Fe doping resulted in enhancement of photocatalytic activity, evaluated by monitoring the degradation of methylene blue solution. 0.8 at% Fe doped TiO_2 films exhibited the highest photocatalytic activity.

1. Introduction

Titanium dioxide (TiO_2) photocatalysts have attracted much interest for air and water purification ever since the discovery of photo-induced water cleavage on TiO_2 electrodes by Fujishima and Honda in the early 1970's. [1]. Dye sensitized solar cells based on TiO_2 is also a subject of interest in the recent years because of their low cost, simple process and environment-friendly photovoltaic ability with good efficiencies compared to conventional silicon solar cells. Also, TiO_2 has long term stability against photo-corrosion and chemical corrosion. Of the two main crystalline polymorphs of TiO_2–rutile and anatase–anatase phase has been widely used as photocatalyst because of its high photo activity. But two factors mainly limit the use of TiO_2 thin films in photocatalytic process: (1) Because of its high band gap, outstanding electronic properties and chemical stability, it can be photoactivated only in the presence of ultraviolet (UV) light, which constitutes less than 5% of total solar energy. Doping with transition metals and non-metallic impurities is a promising route to solve this problem. (2) Electron-hole pairs created undergo very fast recombination, releasing energy in the form of unproductive heat. Hence recombination rate of charge carriers has to be reduced by providing suitable trap states.

To improve the photoactivity of TiO_2, so that absorption threshold can be extended to visible range, transition metals such as Fe, V, Mn, Co and Ni [2–7] can be used as dopants. The transition metal ions can create intermediate energy levels into the band gap of TiO_2. This causes a narrowing of band gap which enables visible light itself to initiate photoactivity. Of these various transition metals Fe is advantageous because of two reasons: (1) the ionic radius of Fe^{3+} (0.064 nm), is very close to that of TiO_2 (0.068 nm) so that Fe^{3+} ions can easily get incorporated into the crystal lattice of TiO_2 and (2) Fe^{3+} ions can act as electron-hole traps and prevent their recombination as the energy level of Fe^{2+}/Fe^{3+} lies close to that of Ti^{3+}/Ti^{4+} [8].

Iron doped TiO_2 (Fe–TiO_2) thin films have been prepared by a variety of techniques such as sol–gel method [9,10], mechanical alloying [11], co-precipitation [12], hydrothermal method [13], controlled hydrolysis [14], metal organic chemical vapor deposition [15] and reactive magnetron sputtering [16,17]. There are varied reports in literature that Fe doped TiO_2 thin films can either increase [12,14,18–21] or decrease [9,22–25] the photocatalytic activity. Also there are diverse reports on the structural patterns such as phase and microstructure of Fe–TiO_2 thin films [26–28]. This has prompted us to undertake further studies on Fe doped TiO_2 thin films. Also radio frequency (RF) magnetron sputtering has the advantages of obtaining uniform large area coatings which have good adherence to the substrate. The present study reports on the structural, optical, photoluminescence and photocatalytic

---

* Corresponding author.
E-mail address: thomaspv_15@yahoo.com (P.V. Thomas).

0040-6090/$ – see front matter © 2013 Elsevier B.V. All rights reserved.
http://dx.doi.org/10.1016/j.tsf.2013.10.112

properties of Fe–TiO_2 thin films deposited on quartz substrates by RF magnetron sputtering.

2. Experimental details

2.1. Preparation of thin films

Pure TiO_2 and Fe_2O_3 (99% Sigma Aldrich) powders were used for target preparation. They were mixed together in the desired proportions and ball milled for 8 h using ball milling apparatus. The sputtering target was prepared by standard ceramic procedure [29]. Six different targets were prepared by changing iron concentration. Fe/Ti atomic ratio in the individual targets was 0, 0.05, 0.1, 0.5. 0.8 and 1.1 at%. The substrate-target distance was 5 cm. Sputtering was carried out at sputtering pressure 1.5 Pa and RF power 120 W for 2 h in pure Ar atmosphere. The films were coated on quartz substrates initially maintained at room temperature. During sputtering, the substrate temperature increased up to 353 K. Post deposition thermal annealing of the films at 873 K was done in air for 2 h. The films thus obtained were coded TO[873], 0.05FTO[873], 0.1FTO[873], 0.5FTO[873], 0.8FTO[873] and 1.1FTO[873] respectively.

2.2. Characterization of thin films

X-ray diffraction (XRD) patterns of the films were recorded using Bruker D8 Advance X-ray diffractometer using Cu Kα radiation ($\lambda = 0.15405$ nm) at a scan rate of $0.05^{o}s^{-1}$. Bragg–Brentano θ–θ configuration was used for the scan. Scanning range was 20 to 60^{o}, and scanning step size was 0.01^{o}. The accelerating voltage and applied current were 40 kV and 40 mA, respectively. The average crystallite size of the film was calculated using Debye–Scherrer formula [30]. The lattice parameters and microstrain of the films were also evaluated [31]. Micro Raman analysis of the films was done using a Labram-HR 800 spectrometer equipped with an argon ion laser. Scanning electron microscopy (SEM) images were recorded using JEOL Model JSM-6390LV microscope equipped with a Energy dispersive spectroscopy (EDX) set up (JEOL Model JED-2300). The accelerating voltage was in the range 20–30 kV for the various films. For EDX measurements, high vacuum resolution of 3 nm was used. Ultraviolet–visible (UV–vis) transmission spectra of the films were recorded using JASCO V-550 spectrophotometer. From the transmission spectra, Swanepoel's envelope method [32] was used to calculate the optical constants and Tauc plot [33] was used to determine the optical band gap of the films. Porosity values were calculated using the relation [34]:

$$P = 1 - \frac{n^2 - 1}{n_d^2 - 1} (\times 100\%)$$

where P is the porosity, n the refractive index of TiO_2 thin film and n_d that of bulk TiO_2. Photoluminescence (PL) spectra of the samples were recorded using PerkinElmer LS 55 spectroflourometer equipped with a 40 W Xenon lamp. Excitation wavelength used was 320 nm.

2.3. Evaluation of photocatalytic activity of thin films

The photoreactor system used in the present study was a rectangular quartz cell (80 × 50 × 3 mm). 20 ml of 0.01 g/l methylene blue (MB) solution was taken in the cell. TiO_2 thin film of dimension 50 × 25 × 1.35 mm was suspended in this solution. The solution was circulated with air during the reaction. The system was irradiated with light from a 125 W high pressure mercury vapor lamp. The irradiation density was 100 mW/cm^2. The photocatalytic experimental setup was kept in dark and the solution was stirred continuously for 30 minutes to ensure adsorption/desorption equilibrium, before irradiation with mercury lamp. This equilibrium concentration was used as the initial value for further photodecomposition process. The absorbance of solution was measured after every half hour, for 2 h. MB has a maximum absorbance at 663 nm. The change in MB concentration with irradiation time was determined by a UV–vis spectrophotometer by measuring its absorbance at 663 nm. Percentage degradation (D) of MB solution was evaluated as follows: $D = (A_0 - A) / A_0 \times 100$ where A_0 is the initial absorbance of the dye solution and A, its absorbance at different irradiation times. The apparent rate constant was also evaluated [35].

3. Results and discussions

3.1. Structural studies

Crystalline structure of pure TiO_2 and Fe–TiO_2 thin films were examined by XRD and micro Raman spectroscopy. Analysis of the XRD and micro Raman spectra are given below:

3.1.1. XRD Studies

Fig. 1 shows the XRD patterns of pure TiO_2 and Fe–TiO_2 thin films post-annealed at 873 K. Pure TiO_2 thin films were XRD-amorphous. But as Fe content was increased, the films exhibited crystallization to anatase (≤0.1 at%) and then to mixed phase (0.5 at%). For the film 0.05FTO[873], two diffraction peaks at $2\theta = 25.3919$ and 37.7948^{o} corresponding to reflections from A(101) and A(004) planes were observed. Four diffraction peaks at $2\theta = 25.2607$, 37.7350, 53.7484 and 55.1023^{o} were observed, corresponding to reflections from A(101), A(004), A(105) and A(211) planes for the film 0.1FTO[873]. In addition to reflections from A(101), A(004), A(200) and A(105) planes at $2\theta = 25.2837$, 37.9356, 48.1654 and 53.6815^{o} respectively, a weak peak corresponding to reflection from R(110) plane at $2\theta = 27.7726^{o}$ was observed in the film 0.5FTO[873]. The 0.8 and 1.1 at% doped Fe–TiO_2 thin films were again amorphous-like in nature. A weak peak corresponding to reflection from A(101) plane was observed at $2\theta = 25.9063^{o}$ for the film 0.8FTO[873]. No preferential orientation along a particular plane was noted in the investigated films. Also, diffraction peaks corresponding to oxides of iron such as FeO, Fe_2O_3, Fe_3O_4 or any mixed oxides such as Fe_xTiO_{2y} were not observed in the XRD patterns. This can be attributed to the fact that most of the Fe ions were inserted into the TiO_2 lattice sites [15].

Also, the intensity of diffraction peaks was found to increase with increasing Fe dopant concentration up to 0.5 at%. This indicates an increase in film crystallinity [28]. But at higher doping concentrations (≥0.5 at%), the films appear amorphous which means crystallinity is

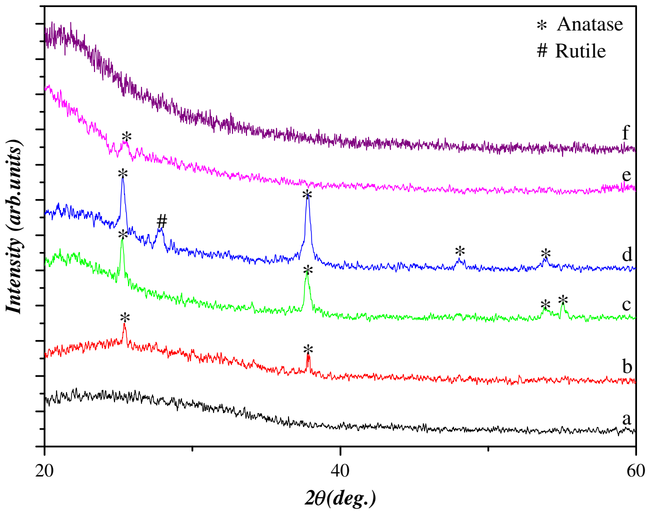

Fig. 1. XRD patterns of (a) pure TiO_2 and (b) 0.05 (c) 0.1 (d) 0.5 (e) 0.8 (f) 1.1 at % Fe–TiO_2 thin films post-annealed at 873 K.